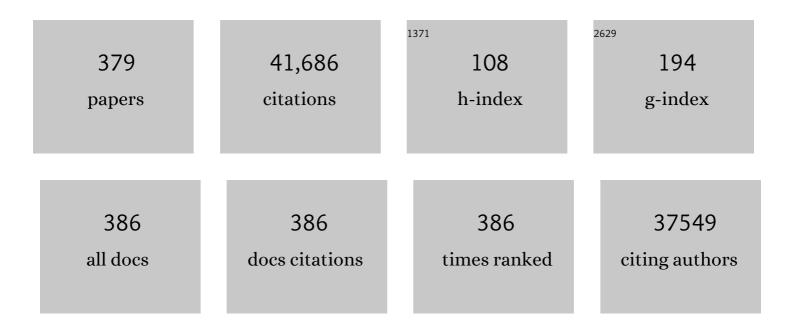
List of Publications by Year in descending order

Source: https://exaly.com/author-pdf/451485/publications.pdf Version: 2024-02-01



#	Article	IF	CITATIONS
1	D-ï€-D molecular layer electronically bridges the NiO hole transport layer and the perovskite layer towards high performance photovoltaics. Journal of Energy Chemistry, 2022, 67, 797-804.	12.9	9
2	Ultrasound-seeded vapor-phase-transport growth of boundary-rich layered double hydroxide nanosheet arrays for highly efficient water splitting. Chemical Engineering Journal, 2022, 433, 134552.	12.7	6
3	Harvesting of Infrared Part of Sunlight to Enhance Polaron Transport and Solar Water Splitting. Advanced Functional Materials, 2022, 32, .	14.9	24
4	New Findings for the Muchâ€Promised Hematite Photoanodes with Gradient Doping and Overlayer Elaboration. Solar Rrl, 2022, 6, .	5.8	15
5	Composition-Tuned Surface Binding on CuZn-Ni Catalysts Boosts CO ₂ RR Selectivity toward CO Generation. , 2022, 4, 497-504.		26
6	Targeted Molecular Design of Functionalized Fullerenes for Highâ€Performance and Stable Perovskite Solar Cells. Small Structures, 2022, 3, .	12.0	17
7	Robotic Hair with Rich Sensation and Piloerection Functionalities Biomimicked by Stimuliâ€Responsive Materials. Advanced Materials Technologies, 2022, 7, .	5.8	2
8	Building Bulk Heterojunction to Enhance Hole Extraction for Highâ€Performance Printable Carbonâ€Based Perovskite Solar Cells. Solar Rrl, 2022, 6, .	5.8	6
9	A visible to near-infrared nanocrystalline organic photodetector with ultrafast photoresponse. Journal of Materials Chemistry C, 2022, 10, 9391-9400.	5.5	8
10	A dual plasmonic core—shell Pt/[TiN@TiO2] catalyst for enhanced photothermal synergistic catalytic activity of VOCs abatement. Nano Research, 2022, 15, 7071-7080.	10.4	17
11	Bipolar dual-broadband photodetectors based on perovskite heterojunctions. Nano Futures, 2022, 6, 025006.	2.2	2
12	A Heatâ€Liquefiable Solid Precursor for Ambient Growth of Perovskites with High Tunability, Performance and Stability. Small Methods, 2022, 6, .	8.6	4
13	Targeted Molecular Design of Functionalized Fullerenes for Highâ€Performance and Stable Perovskite Solar Cells. Small Structures, 2022, 3, .	12.0	3
14	Cu Vacancy Induced Product Switching from Formate to CO for CO ₂ Reduction on Copper Sulfide. ACS Catalysis, 2022, 12, 9074-9082.	11.2	35
15	Crystallization Kinetics Modulation of FASnI ₃ Films with Preâ€nucleation Clusters for Efficient Leadâ€Free Perovskite Solar Cells. Angewandte Chemie - International Edition, 2021, 60, 3693-3698.	13.8	80
16	Tuning SAPO-34 with a tailor-designed zwitterionic amino acid for improved MTO performance. Microporous and Mesoporous Materials, 2021, 310, 110590.	4.4	10
17	Crystallization Kinetics Modulation of FASnI ₃ Films with Preâ€nucleation Clusters for Efficient Leadâ€Free Perovskite Solar Cells. Angewandte Chemie, 2021, 133, 3737-3742.	2.0	20
18	Selfâ€Driven Perovskite Narrowband Photodetectors with Tunable Spectral Responses. Advanced Materials, 2021, 33, e2005557.	21.0	109

#	Article	IF	CITATIONS
19	Atomically targeting NiFe LDH to create multivacancies for OER catalysis with a small organic anchor. Nano Energy, 2021, 81, 105606.	16.0	204
20	Formation of FeOOH Nanosheets Induces Substitutional Doping of CeO _{2â^'} <i>_x</i> with Highâ€Valence Ni for Efficient Water Oxidation. Advanced Energy Materials, 2021, 11, 2002731.	19.5	110
21	Recent advances in surface/interface engineering of noble-metal free catalysts for energy conversion reactions. Materials Chemistry Frontiers, 2021, 5, 3576-3592.	5.9	9
22	Surface passivation of organometal halide perovskites by atomic layer deposition: an investigation of the mechanism of efficient inverted planar solar cells. Nanoscale Advances, 2021, 3, 2305-2315.	4.6	25
23	Highly efficient and stable broadband near-infrared-emitting lead-free metal halide double perovskites. Journal of Materials Chemistry C, 2021, 9, 13474-13483.	5.5	13
24	Discovery of a New Intermediate Enables One‣tep Deposition of Highâ€Quality Perovskite Films via Solvent Engineering. Solar Rrl, 2021, 5, 2000712.	5.8	24
25	TM LDH Meets Birnessite: A 2Dâ€2D Hybrid Catalyst with Longâ€Term Stability for Water Oxidation at Industrial Operating Conditions. Angewandte Chemie - International Edition, 2021, 60, 9699-9705.	13.8	57
26	An aerosol-liquid-solid process for the general synthesis of halide perovskite thick films for direct-conversion X-ray detectors. Matter, 2021, 4, 942-954.	10.0	80
27	TM LDH Meets Birnessite: A 2Dâ€2D Hybrid Catalyst with Longâ€Term Stability for Water Oxidation at Industrial Operating Conditions. Angewandte Chemie, 2021, 133, 9785-9791.	2.0	3
28	Ambient Inkjetâ€Printed Highâ€Efficiency Perovskite Solar Cells: Manipulating the Spreading and Crystallization Behaviors of Picoliter Perovskite Droplets. Solar Rrl, 2021, 5, 2100106.	5.8	24
29	Redirecting dynamic surface restructuring of a layered transition metal oxide catalyst for superior water oxidation. Nature Catalysis, 2021, 4, 212-222.	34.4	266
30	Dual–Functionalâ€Polymer Dopant–Passivant Boosted Electron Transport Layer for Highâ€Performance Inverted Perovskite Solar Cells. Solar Rrl, 2021, 5, 2100236.	5.8	5
31	Selfâ€Driven Perovskite Dualâ€Band Photodetectors Enabled by a Charge Separation Reversion Mechanism. Advanced Optical Materials, 2021, 9, 2100517.	7.3	21
32	Organic metal-free halide perovskites tuned up for X-ray detection. Matter, 2021, 4, 2111-2114.	10.0	7
33	Conductive Polymer Intercalation Tunes Charge Transfer and Sorption–Desorption Properties of LDH Enabling Efficient Alkaline Water Oxidation. ACS Applied Materials & Interfaces, 2021, 13, 37063-37070.	8.0	19
34	Mini Review on Active Sites in Ce-Based Electrocatalysts for Alkaline Water Splitting. Energy & Fuels, 2021, 35, 19000-19011.	5.1	34
35	Activating Metal Oxides Nanocatalysts for Electrocatalytic Water Oxidation by Quenching-Induced Near-Surface Metal Atom Functionality. Journal of the American Chemical Society, 2021, 143, 14169-14177.	13.7	101
36	Plasmonic Hot Hole Extraction from CuS Nanodisks Enables Significant Acceleration of Oxygen Evolution Reactions. Journal of Physical Chemistry Letters, 2021, 12, 7988-7996.	4.6	14

#	Article	lF	CITATIONS
37	Sequential Growth of 2D/3D Double‣ayer Perovskite Films with Superior Xâ€Ray Detection Performance. Advanced Science, 2021, 8, e2102730.	11.2	55
38	Multifunctional Molecular Design of a New Fulleropyrrolidine Electron Transport Material Family Engenders High Performance of Perovskite Solar Cells. Advanced Functional Materials, 2021, 31, 2107695.	14.9	17
39	Controlling the Crystallization Kinetics of Leadâ€Free Tin Halide Perovskites for High Performance Green Photovoltaics. Advanced Energy Materials, 2021, 11, 2102131.	19.5	47
40	Boosting performance and stability of inverted perovskite solar cells by modulating the cathode interface with phenyl phosphine-inlaid semiconducting polymer. Nano Energy, 2021, 89, 106374.	16.0	10
41	Boosting the electrochemical performance of hematite nanorods <i>via</i> quenching-induced metal single atom functionalization. Journal of Materials Chemistry A, 2021, 9, 3492-3499.	10.3	20
42	Trap-Assisted Charge Storage in Titania Nanocrystals toward Optoelectronic Nonvolatile Memory. Nano Letters, 2021, 21, 723-730.	9.1	20
43	High throughput screening of novel tribromide perovskite materials for high-photovoltage solar cells. Journal of Materials Chemistry A, 2021, 9, 25502-25512.	10.3	8
44	Activating Carbon Nitride by BP@Ni for the Enhanced Photocatalytic Hydrogen Evolution and Selective Benzyl Alcohol Oxidation. ACS Applied Materials & Interfaces, 2021, 13, 50988-50995.	8.0	14
45	Nucleophilic Etching Growth of Zeolite Materials with High Tunability. Advanced Materials Interfaces, 2021, 8, .	3.7	2
46	Unexpected high selectivity for acetate formation from CO ₂ reduction with copper based 2D hybrid catalysts at ultralow potentials. Chemical Science, 2021, 12, 15382-15388.	7.4	19
47	Controlling Apparent Coordinated Solvent Number in the Perovskite Intermediate Phase Film for Developing Largeâ€Area Perovskite Solar Modules. Energy Technology, 2020, 8, 1900972.	3.8	9
48	Interfacial Postâ€Treatment for Enhancing the Performance of Printable Carbonâ€Based Perovskite Solar Cells. Solar Rrl, 2020, 4, 1900278.	5.8	23
49	Material and Interface Engineering for Highâ€Performance Perovskite Solar Cells: A Personal Journey and Perspective. Chemical Record, 2020, 20, 209-229.	5.8	9
50	Interfacial effects in hierarchically porous α-MnO2/Mn3O4 heterostructures promote photocatalytic oxidation activity. Applied Catalysis B: Environmental, 2020, 268, 118418.	20.2	100
51	Recent advances in transition metal based compound catalysts for water splitting from the perspective of crystal engineering. CrystEngComm, 2020, 22, 1531-1540.	2.6	32
52	NiMn compound nanosheets for electrocatalytic water oxidation: effects of atomic structures and oxidation states. Nanoscale, 2020, 12, 2472-2478.	5.6	17
53	Highly efficient tin perovskite solar cells achieved in a wide oxygen concentration range. Journal of Materials Chemistry A, 2020, 8, 2760-2768.	10.3	85
54	Efficient and stable tin-based perovskite solar cells by introducing π-conjugated Lewis base. Science China Chemistry, 2020, 63, 107-115.	8.2	160

#	ŧ	Article	IF	CITATIONS
5	5	Kineticâ€Oriented Construction of MoS ₂ Synergistic Interface to Boost pHâ€Universal Hydrogen Evolution. Advanced Functional Materials, 2020, 30, 1908520.	14.9	59
5	6	Ion Migration: A "Doubleâ€Edged Sword―for Halideâ€Perovskiteâ€Based Electronic Devices. Small Methods, 2020, 4, 1900552.	8.6	127
5	7	Optically Stimulated Luminescence Phosphors: Principles, Applications, and Prospects. Laser and Photonics Reviews, 2020, 14, 2000123.	8.7	73
5	8	A dramatic conformational effect of multifunctional zwitterions on zeolite crystallization. Chemical Communications, 2020, 56, 14693-14696.	4.1	1
5	9	Identifying the Active Sites of a Single Atom Catalyst with pH-Universal Oxygen Reduction Reaction Activity. Cell Reports Physical Science, 2020, 1, 100115.	5.6	26
6	60	Surface Sulfuration of NiO Boosts the Performance of Inverted Perovskite Solar Cells. Solar Rrl, 2020, 4, 2000270.	5.8	31
6	51	The Role of Ceria in a Hybrid Catalyst toward Alkaline Water Oxidation. ChemSusChem, 2020, 13, 5273-5279.	6.8	36
6	62	Halide perovskites: A dark horse for direct Xâ€ray imaging. EcoMat, 2020, 2, e12064.	11.9	84
6	63	Templated growth of FASnI ₃ crystals for efficient tin perovskite solar cells. Energy and Environmental Science, 2020, 13, 2896-2902.	30.8	165
6	64	Aliovalent Doping and Surface Grafting Enable Efficient and Stable Leadâ€Free Blueâ€Emitting Perovskite Derivative. Advanced Optical Materials, 2020, 8, 2000779.	7.3	68
6	5	Non-precious-metal catalysts for alkaline water electrolysis: <i>operando</i> characterizations, theoretical calculations, and recent advances. Chemical Society Reviews, 2020, 49, 9154-9196.	38.1	448
6	6	NaBH ₄ induces a high ratio of Ni ³⁺ /Ni ²⁺ boosting OER activity of the NiFe LDH electrocatalyst. RSC Advances, 2020, 10, 33475-33482.	3.6	62
6	67	Anomalous Photoinduced Reconstructing and Dark Self-Healing Processes on Bi ₂ O ₂ S Nanoplates. Journal of Physical Chemistry Letters, 2020, 11, 7832-7838.	4.6	7
6	8	A zeolite-based ship-in-a-bottle route to ultrasmall carbon dots for live cell labeling and bioimaging. Nanoscale Advances, 2020, 2, 5803-5809.	4.6	7
6	9	Effect of Absorbed Sulfate Poisoning on the Performance of Catalytic Oxidation of VOCs over MnO ₂ . ACS Applied Materials & amp; Interfaces, 2020, 12, 50566-50572.	8.0	36
7	0	Potassiumâ€Induced Phase Stability Enables Stable and Efficient Wideâ€Bandgap Perovskite Solar Cells. Solar Rrl, 2020, 4, 2000098.	5.8	37
7.	1	Efficient and stable tin perovskite solar cells enabled by amorphous-polycrystalline structure. Nature Communications, 2020, 11, 2678.	12.8	143
7	2	Surface-Controlled Oriented Growth of FASnI3 Crystals for Efficient Lead-free Perovskite Solar Cells. Joule, 2020, 4, 902-912.	24.0	208

#	Article	IF	CITATIONS
73	Good or evil: what is the role of water in crystallization of organometal halide perovskites?. Nanoscale Horizons, 2020, 5, 1147-1154.	8.0	11
74	<i>In situ</i> growth of Fe2WO6 on WO3 nanosheets to fabricate heterojunction arrays for boosting solar water splitting. Journal of Chemical Physics, 2020, 152, 214704.	3.0	19
75	Efficient and Stable Tin Perovskite Solar Cells Enabled by Graded Heterostructure of Lightâ€Absorbing Layer. Solar Rrl, 2020, 4, 2000240.	5.8	53
76	Highly Reproducible and Efficient FASnI ₃ Perovskite Solar Cells Fabricated with Volatilizable Reducing Solvent. Journal of Physical Chemistry Letters, 2020, 11, 2965-2971.	4.6	115
77	<i>In situ</i> templating synthesis of mesoporous Ni–Fe electrocatalyst for oxygen evolution reaction. RSC Advances, 2020, 10, 23321-23330.	3.6	11
78	Gaining Insight into the Effect of Organic Interface Layer on Suppressing Ion Migration Induced Interfacial Degradation in Perovskite Solar Cells. Advanced Functional Materials, 2020, 30, 2000837.	14.9	29
79	An amorphous trimetallic (Ni–Co–Fe) hydroxide-sheathed 3D bifunctional electrode for superior oxygen evolution and high-performance cable-type flexible zinc–air batteries. Journal of Materials Chemistry A, 2020, 8, 5601-5611.	10.3	57
80	A prenucleation strategy for ambient fabrication of perovskite solar cells with high device performance uniformity. Nature Communications, 2020, 11, 1006.	12.8	98
81	Harnessing hierarchical architectures to trap light for efficient photoelectrochemical cells. Energy and Environmental Science, 2020, 13, 660-684.	30.8	43
82	Cation Diffusion Guides Hybrid Halide Perovskite Crystallization during the Gel Stage. Angewandte Chemie, 2020, 132, 6035-6043.	2.0	22
83	Cation Diffusion Guides Hybrid Halide Perovskite Crystallization during the Gel Stage. Angewandte Chemie - International Edition, 2020, 59, 5979-5987.	13.8	29
84	Recent advances in white light-emitting diodes of carbon quantum dots. Nanoscale, 2020, 12, 4826-4832.	5.6	98
85	Graded 2D/3D Perovskite Heterostructure for Efficient and Operationally Stable MAâ€Free Perovskite Solar Cells. Advanced Materials, 2020, 32, e2000571.	21.0	166
86	(Invited) Nanostructured Photoelectrochemical Electrodes and Electrocatalysts for Efficient Solar Energy Conversion. ECS Meeting Abstracts, 2020, MA2020-02, 3092-3092.	0.0	0
87	An Ultraâ€low Concentration of Gold Nanoparticles Embedded in the NiO Hole Transport Layer Boosts the Performance of pâ€iâ€n Perovskite Solar Cells. Solar Rrl, 2019, 3, 1800278.	5.8	38
88	Enhancing photoelectrochemical water splitting by combining work function tuning and heterojunction engineering. Nature Communications, 2019, 10, 3687.	12.8	300
89	Dispersing transition metal vacancies in layered double hydroxides by ionic reductive complexation extraction for efficient water oxidation. Chemical Science, 2019, 10, 8354-8359.	7.4	54
90	Highly Stable and Efficient FASnI ₃ â€Based Perovskite Solar Cells by Introducing Hydrogen Bonding. Advanced Materials, 2019, 31, e1903721.	21.0	266

#	Article	IF	CITATIONS
91	Freeing the Polarons to Facilitate Charge Transport in BiVO ₄ from Oxygen Vacancies with an Oxidative 2D Precursor. Angewandte Chemie - International Edition, 2019, 58, 19087-19095.	13.8	64
92	Hydrogen Evolution Reaction: Oneâ€Step Controllable Synthesis of Catalytic Ni ₄ Mo/MoO <i>_x</i> /Cu Nanointerfaces for Highly Efficient Water Reduction (Adv. Energy Mater. 41/2019). Advanced Energy Materials, 2019, 9, 1970162.	19.5	0
93	Accelerating the Screening of Perovskite Compositions for Photovoltaic Applications through Highâ€Throughput Inkjet Printing. Advanced Functional Materials, 2019, 29, 1905487.	14.9	37
94	One‣tep Controllable Synthesis of Catalytic Ni ₄ Mo/MoO <i>_x</i> /Cu Nanointerfaces for Highly Efficient Water Reduction. Advanced Energy Materials, 2019, 9, 1901454.	19.5	39
95	Freeing the Polarons to Facilitate Charge Transport in BiVO ₄ from Oxygen Vacancies with an Oxidative 2D Precursor. Angewandte Chemie, 2019, 131, 19263-19271.	2.0	21
96	Fluorescence–phosphorescence dual emissive carbon nitride quantum dots show 25% white emission efficiency enabling single-component WLEDs. Chemical Science, 2019, 10, 9801-9806.	7.4	115
97	Tailoring Multidimensional Traps for Rewritable Multilevel Optical Data Storage. ACS Applied Materials & Interfaces, 2019, 11, 35023-35029.	8.0	56
98	One-pot synthesis of manganese oxides and cobalt phosphides nanohybrids with abundant heterointerfaces in an amorphous matrix for efficient hydrogen evolution in alkaline solution. Journal of Materials Chemistry A, 2019, 7, 22530-22538.	10.3	32
99	Polyethyleneimine-functionalized carbon nanotubes as an interlayer to bridge perovskite/carbon for all inorganic carbon-based perovskite solar cells. Journal of Materials Chemistry A, 2019, 7, 22005-22011.	10.3	47
100	Skillfully deflecting the question: a small amount of piperazine-1,4-diium iodide radically enhances the thermal stability of CsPbI ₃ perovskite. Journal of Materials Chemistry C, 2019, 7, 11757-11763.	5.5	32
101	Defect-Rich NiCeO _{<i>x</i>} Electrocatalyst with Ultrahigh Stability and Low Overpotential for Water Oxidation. ACS Catalysis, 2019, 9, 1605-1611.	11.2	113
102	Surface Thermolytic Behavior of Nickel Amidinate and Its Implication on the Atomic Layer Deposition of Nickel Compounds. Chemistry of Materials, 2019, 31, 5172-5180.	6.7	17
103	Methods and strategies for achieving high-performance carbon-based perovskite solar cells without hole transport materials. Journal of Materials Chemistry A, 2019, 7, 15476-15490.	10.3	85
104	Toward Efficient Charge Collection and Light Absorption: A Perspective of Light Trapping for Advanced Photoelectrodes. Journal of Physical Chemistry C, 2019, 123, 18753-18770.	3.1	12
105	Highly efficient and stable white LEDs based on pure red narrow bandwidth emission triangular carbon quantum dots for wide-color gamut backlight displays. Nano Research, 2019, 12, 1669-1674.	10.4	107
106	Organic Mesopore Generating Agents (OMeGAs) for Hierarchical Zeolites: Combining Functions on Multiple Scales. ChemNanoMat, 2019, 5, 869-877.	2.8	8
107	Carbon quantum dots: an emerging material for optoelectronic applications. Journal of Materials Chemistry C, 2019, 7, 6820-6835.	5.5	225
108	Cation and anion immobilization through chemical bonding enhancement with fluorides for stable halide perovskite solar cells. Nature Energy, 2019, 4, 408-415.	39.5	831

#	Article	IF	CITATIONS
109	Designing a Perylene Diimide/Fullerene Hybrid as Effective Electron Transporting Material in Inverted Perovskite Solar Cells with Enhanced Efficiency and Stability. Angewandte Chemie, 2019, 131, 8608.	2.0	14
110	Designing a Perylene Diimide/Fullerene Hybrid as Effective Electron Transporting Material in Inverted Perovskite Solar Cells with Enhanced Efficiency and Stability. Angewandte Chemie - International Edition, 2019, 58, 8520-8525.	13.8	73
111	Efficient and Stable CsPbl ₃ Solar Cells via Regulating Lattice Distortion with Surface Organic Terminal Groups. Advanced Materials, 2019, 31, e1900605.	21.0	209
112	Ultrabroad-band, red sufficient, solid white emission from carbon quantum dot aggregation for single component warm white light emitting diodes with a 91 high color rendering index. Chemical Communications, 2019, 55, 6531-6534.	4.1	62
113	Natrium Doping Pushes the Efficiency of Carbon-Based CsPbI3 Perovskite Solar Cells to 10.7%. IScience, 2019, 15, 156-164.	4.1	81
114	Electroluminescent Warm White Lightâ€Emitting Diodes Based on Passivation Enabled Bright Red Bandgap Emission Carbon Quantum Dots. Advanced Science, 2019, 6, 1900397.	11.2	174
115	Materials and structures for the electron transport layer of efficient and stable perovskite solar cells. Science China Chemistry, 2019, 62, 800-809.	8.2	59
116	Understanding the Diverse Coordination Modes of Thiocyanate Anion on Solid Surfaces. Journal of Physical Chemistry C, 2019, 123, 9282-9291.	3.1	10
117	Efficient Defect Passivation for Perovskite Solar Cells by Controlling the Electron Density Distribution of Donorâ€i€â€Acceptor Molecules. Advanced Energy Materials, 2019, 9, 1803766.	19.5	280
118	Solution-processed electron transport layer of n-doped fullerene for efficient and stable all carbon based perovskite solar cells. Journal of Materials Chemistry A, 2019, 7, 7710-7716.	10.3	29
119	3D Hierarchical Nanorod@Nanobowl Array Photoanode with a Tunable Lightâ€Trapping Cutoff and Bottomâ€Selective Field Enhancement for Efficient Solar Water Splitting. Small, 2019, 15, e1804976.	10.0	14
120	Zwitterion Coordination Induced Highly Orientational Order of CH ₃ NH ₃ PbI ₃ Perovskite Film Delivers a High Open Circuit Voltage Exceeding 1.2 V. Advanced Functional Materials, 2019, 29, 1901026.	14.9	134
121	Water Splitting: 3D Hierarchical Nanorod@Nanobowl Array Photoanode with a Tunable Lightâ€Trapping Cutoff and Bottomâ€Selective Field Enhancement for Efficient Solar Water Splitting (Small 14/2019). Small, 2019, 15, 1970074.	10.0	0
122	Lowâ€Temperature In Situ Amino Functionalization of TiO ₂ Nanoparticles Sharpens Electron Management Achieving over 21% Efficient Planar Perovskite Solar Cells. Advanced Materials, 2019, 31, e1806095.	21.0	194
123	Strain engineering in perovskite solar cells and its impacts on carrier dynamics. Nature Communications, 2019, 10, 815.	12.8	528
124	Spacer layer design for efficient fully printable mesoscopic perovskite solar cells. RSC Advances, 2019, 9, 29840-29846.	3.6	14
125	Suppressing the carrier concentration of zinc tin nitride thin films by excess zinc content and low temperature growth. Applied Physics Letters, 2019, 115, .	3.3	14
126	From One to Two: In Situ Construction of an Ultrathin 2D-2D Closely Bonded Heterojunction from a Single-Phase Monolayer Nanosheet. Journal of the American Chemical Society, 2019, 141, 19715-19727.	13.7	148

#	Article	IF	CITATIONS
127	HxMoO3â^'ynanobelts: an excellent alternative to carbon electrodes for high performance mesoscopic perovskite solar cells. Journal of Materials Chemistry A, 2019, 7, 1499-1508.	10.3	8
128	Excess Cesium Iodide Induces Spinodal Decomposition of CsPbI ₂ Br Perovskite Films. Journal of Physical Chemistry Letters, 2019, 10, 194-199.	4.6	69
129	An Ultrathin Ferroelectric Perovskite Oxide Layer for Highâ€Performance Hole Transport Material Free Carbon Based Halide Perovskite Solar Cells. Advanced Functional Materials, 2019, 29, 1806506.	14.9	93
130	Ultrastable and Lowâ€Threshold Random Lasing from Narrowâ€Bandwidthâ€Emission Triangular Carbon Quantum Dots. Advanced Optical Materials, 2019, 7, 1801202.	7.3	67
131	Three-Dimensional Decoupling Co-Catalyst from a Photoabsorbing Semiconductor as a New Strategy To Boost Photoelectrochemical Water Splitting. Nano Letters, 2019, 19, 455-460.	9.1	52
132	Solution Grown Single-Unit-Cell Quantum Wires Affording Self-Powered Solar-Blind UV Photodetectors with Ultrahigh Selectivity and Sensitivity. Journal of the American Chemical Society, 2019, 141, 3480-3488.	13.7	44
133	Epitaxial Growth of Iron Tungstate Nanosheets on One-Dimensional Photoanodes for Efficient Solar Water Oxidation. ECS Meeting Abstracts, 2019, , .	0.0	0
134	Ultrasonic Spray Pyrolysis Deposition of NiO Thin Film for Efficient Perovskite Solar Cell. ECS Meeting Abstracts, 2019, , .	0.0	0
135	Versatility of Carbon Enables All Carbon Based Perovskite Solar Cells to Achieve High Efficiency and High Stability. Advanced Materials, 2018, 30, e1706975.	21.0	95
136	Ultrathin amorphous cobalt–vanadium hydr(oxy)oxide catalysts for the oxygen evolution reaction. Energy and Environmental Science, 2018, 11, 1736-1741.	30.8	310
137	Inorganic Perovskite Solar Cells: A Rapidly Growing Field. Solar Rrl, 2018, 2, 1700188.	5.8	193
138	Lowâ€Temperature Solutionâ€Processed CuCrO ₂ Holeâ€Transporting Layer for Efficient and Photostable Perovskite Solar Cells. Advanced Energy Materials, 2018, 8, 1702762.	19.5	137
139	Hydrogen evolution reactions boosted by bridge bonds between electrocatalysts and electrodes. Nanoscale, 2018, 10, 4068-4076.	5.6	10
140	Enhancing Full Water-Splitting Performance of Transition Metal Bifunctional Electrocatalysts in Alkaline Solutions by Tailoring CeO ₂ –Transition Metal Oxides–Ni Nanointerfaces. ACS Energy Letters, 2018, 3, 290-296.	17.4	152
141	The Flexibility of an Amorphous Cobalt Hydroxide Nanomaterial Promotes the Electrocatalysis of Oxygen Evolution Reaction. Small, 2018, 14, e1703514.	10.0	121
142	Nanotextured Spikes of α-Fe ₂ O ₃ /NiFe ₂ O ₄ Composite for Efficient Photoelectrochemical Oxidation of Water. Langmuir, 2018, 34, 3555-3564.	3.5	31
143	Exploratory Study of Zn _{<i>x</i>} PbO _{<i>y</i>} Photoelectrodes for Unassisted Overall Solar Water Splitting. ACS Applied Materials & Interfaces, 2018, 10, 10918-10926.	8.0	7
144	Interface Engineering for Highly Efficient and Stable Planar pâ€iâ€n Perovskite Solar Cells. Advanced Energy Materials, 2018, 8, 1701883.	19.5	338

#	Article	IF	CITATIONS
145	(Keynote) One-Pot Synthesis of Manganese Oxides and Cobalt Phosphides Nanohybrids with Abundant Hetero-Interfaces in Amorphous Matrix for Efficient Hydrogen Evolution in Alkaline Solution. ECS Transactions, 2018, 88, 381-397.	0.5	0
146	Wurtzite CoO: a direct band gap oxide suitable for a photovoltaic absorber. Chemical Communications, 2018, 54, 13949-13952.	4.1	21
147	Effects of Metal Combinations on the Electrocatalytic Properties of Transition-Metal-Based Layered Double Hydroxides for Water Oxidation: A Perspective with Insights. ACS Omega, 2018, 3, 16529-16541.	3.5	42
148	Boosting the Photoelectrochemical Water Oxidation at Hematite Photoanode by Innovating a Hierarchical Ball-on-Wire-Array Structure. ACS Applied Energy Materials, 2018, 1, 5836-5841.	5.1	9
149	Sequential precipitation induced interdiffusion: a general strategy to synthesize microtubular materials for high performance lithium ion battery electrodes. Journal of Materials Chemistry A, 2018, 6, 18430-18437.	10.3	12
150	Efficient, Scalable, and Highâ€Temperature Selective Solar Absorbers Based on Hybridâ€Strategy Plasmonic Metamaterials. Solar Rrl, 2018, 2, 1800057.	5.8	48
151	Molecular design enabled reduction of interface trap density affords highly efficient and stable perovskite solar cells with over 83% fill factor. Nano Energy, 2018, 52, 300-306.	16.0	112
152	Efficient, Scalable, and Highâ€Temperature Selective Solar Absorbers Based on Hybridâ€Strategy Plasmonic Metamaterials (Solar RRL 8â^•2018). Solar Rrl, 2018, 2, 1870196.	5.8	7
153	Engineering triangular carbon quantum dots with unprecedented narrow bandwidth emission for multicolored LEDs. Nature Communications, 2018, 9, 2249.	12.8	676
154	Engineering Stepped Edge Surface Structures of MoS2 Sheet Stacks to Accelerate the Hydrogen Evolution Reaction. ECS Meeting Abstracts, 2018, , .	0.0	0
155	(Keynote) Nanomaterials and Interfaces for Efficient Solar Energy Conversion. ECS Meeting Abstracts, 2018, , .	0.0	0
156	Carbon quantum dots as a visible light sensitizer to significantly increase the solar water splitting performance of bismuth vanadate photoanodes. Energy and Environmental Science, 2017, 10, 772-779.	30.8	315
157	Lightâ€Emitting Diodes: Bright Multicolor Bandgap Fluorescent Carbon Quantum Dots for Electroluminescent Lightâ€Emitting Diodes (Adv. Mater. 3/2017). Advanced Materials, 2017, 29, .	21.0	5
158	Carbonâ€Based Perovskite Solar Cells without Hole Transport Materials: The Front Runner to the Market?. Advanced Materials, 2017, 29, 1603994.	21.0	261
159	Hydrogen evolution electrocatalysis with binary-nonmetal transition metal compounds. Journal of Materials Chemistry A, 2017, 5, 5995-6012.	10.3	142
160	A pure and stable intermediate phase is key to growing aligned and vertically monolithic perovskite crystals for efficient PIN planar perovskite solar cells with high processibility and stability. Nano Energy, 2017, 34, 58-68.	16.0	151
161	Nitrogenâ€Doped Co ₃ O ₄ Mesoporous Nanowire Arrays as an Additiveâ€Free Airâ€Cathode for Flexible Solidâ€State Zinc–Air Batteries. Advanced Materials, 2017, 29, 1602868.	21.0	428
162	Unveiling a Key Intermediate in Solvent Vapor Postannealing to Enlarge Crystalline Domains of Organometal Halide Perovskite Films. Advanced Functional Materials, 2017, 27, 1604944.	14.9	107

#	Article	IF	CITATIONS
163	Constructing three-dimensional porous Ni/Ni ₃ S ₂ nano-interfaces for hydrogen evolution electrocatalysis under alkaline conditions. Dalton Transactions, 2017, 46, 10700-10706.	3.3	41
164	Solar Cells: Dual Interfacial Modifications Enable High Performance Semitransparent Perovskite Solar Cells with Large Open Circuit Voltage and Fill Factor (Adv. Energy Mater. 9/2017). Advanced Energy Materials, 2017, 7, .	19.5	1
165	Profiling the organic cation-dependent degradation of organolead halide perovskite solar cells. Journal of Materials Chemistry A, 2017, 5, 1103-1111.	10.3	155
166	Antipulverization Electrode Based on Lowâ€Carbon Tripleâ€Shelled Superstructures for Lithiumâ€Ion Batteries. Advanced Materials, 2017, 29, 1701494.	21.0	92
167	Fullyâ€Inorganic Trihalide Perovskite Nanocrystals: A New Research Frontier of Optoelectronic Materials. Advanced Materials, 2017, 29, 1700775.	21.0	230
168	Morphology onserved Transformations of Metalâ€Based Precursors to Hierarchically Porous Microâ€∤Nanostructures for Electrochemical Energy Conversion and Storage. Advanced Materials, 2017, 29, 1607015.	21.0	79
169	Boron Doping of Multiwalled Carbon Nanotubes Significantly Enhances Hole Extraction in Carbon-Based Perovskite Solar Cells. Nano Letters, 2017, 17, 2496-2505.	9.1	184
170	Dual Interfacial Modifications Enable High Performance Semitransparent Perovskite Solar Cells with Large Open Circuit Voltage and Fill Factor. Advanced Energy Materials, 2017, 7, 1602333.	19.5	209
171	Engineering stepped edge surface structures of MoS ₂ sheet stacks to accelerate the hydrogen evolution reaction. Energy and Environmental Science, 2017, 10, 593-603.	30.8	284
172	Low-temperature aqueous solution processed ZnO as an electron transporting layer for efficient perovskite solar cells. Materials Chemistry Frontiers, 2017, 1, 802-806.	5.9	25
173	Self-driven hematite-based photoelectrochemical water splitting cells with three-dimensional nanobowl heterojunction and high-photovoltage perovskite solar cells. Materials Today Energy, 2017, 6, 128-135.	4.7	23
174	Pinning Down the Anomalous Light Soaking Effect toward High-Performance and Fast-Response Perovskite Solar Cells: The Ion-Migration-Induced Charge Accumulation. Journal of Physical Chemistry Letters, 2017, 8, 5069-5076.	4.6	60
175	Nanohybridization of MoS2 with Layered Double Hydroxides Efficiently Synergizes the Hydrogen Evolution in Alkaline Media. Joule, 2017, 1, 383-393.	24.0	386
176	Tuning the A-site cation composition of FA perovskites for efficient and stable NiO-based p–i–n perovskite solar cells. Journal of Materials Chemistry A, 2017, 5, 21858-21865.	10.3	39
177	Dimensional Engineering of a Graded 3D–2D Halide Perovskite Interface Enables Ultrahigh <i>V</i> _{oc} Enhanced Stability in the pâ€iâ€n Photovoltaics. Advanced Energy Materials, 2017, 7, 1701038.	19.5	319
178	Stabilizing and scaling up carbon-based perovskite solar cells. Journal of Materials Research, 2017, 32, 3011-3020.	2.6	30
179	53% Efficient Red Emissive Carbon Quantum Dots for High Color Rendering and Stable Warm Whiteâ€Lightâ€Emitting Diodes. Advanced Materials, 2017, 29, 1702910.	21.0	563
180	Integration of inverse nanocone array based bismuth vanadate photoanodes and bandgap-tunable perovskite solar cells for efficient self-powered solar water splitting. Journal of Materials Chemistry A, 2017, 5, 19091-19097.	10.3	55

#	Article	IF	CITATIONS
181	Ultrasound-spray deposition of multi-walled carbon nanotubes on NiO nanoparticles-embedded perovskite layers for high-performance carbon-based perovskite solar cells. Nano Energy, 2017, 42, 322-333.	16.0	82
182	Exceptionally High Payload of the IR780 Iodide on Folic Acid-Functionalized Graphene Quantum Dots for Targeted Photothermal Therapy. ACS Applied Materials & Interfaces, 2017, 9, 22332-22341.	8.0	167
183	Strategies for Improving Efficiency and Stability of Perovskite Solar Cells. MRS Advances, 2017, 2, 3051-3060.	0.9	3
184	Hydrolysis-Coupled Redox Reaction to 3D Cu/Fe ₃ O ₄ Nanorod Array Electrodes for High-Performance Lithium-Ion Batteries. Inorganic Chemistry, 2017, 56, 7657-7667.	4.0	17
185	Bright Multicolor Bandgap Fluorescent Carbon Quantum Dots for Electroluminescent Lightâ€Emitting Diodes. Advanced Materials, 2017, 29, 1604436.	21.0	643
186	(Invited) Novel Nanomaterials, Structures and Interfaces for Solar Fuel Production. ECS Meeting Abstracts, 2017, , .	0.0	0
187	Effects of a Molecular Monolayer Modification of NiO Nanocrystal Layer Surfaces on Perovskite Crystallization and Interface Contact toward Faster Hole Extraction and Higher Photovoltaic Performance. Advanced Functional Materials, 2016, 26, 2950-2958.	14.9	305
188	Enhanced Efficiency and Stability of Inverted Perovskite Solar Cells Using Highly Crystalline SnO ₂ Nanocrystals as the Robust Electronâ€Transporting Layer. Advanced Materials, 2016, 28, 6478-6484.	21.0	447
189	Dualâ€Ðoped Molybdenum Trioxide Nanowires: A Bifunctional Anode for Fiber‧haped Asymmetric Supercapacitors and Microbial Fuel Cells. Angewandte Chemie, 2016, 128, 6874-6878.	2.0	70
190	Solvent Engineering Boosts the Efficiency of Paintable Carbonâ€Based Perovskite Solar Cells to Beyond 14%. Advanced Energy Materials, 2016, 6, 1502087.	19.5	306
191	High Performance Perovskite Solar Cells through Surface Modification, Mixed Solvent Engineering and Nanobowl-Assisted Light Harvesting. MRS Advances, 2016, 1, 3175-3184.	0.9	9
192	Fabrication of CuFe ₂ O ₄ /α-Fe ₂ O ₃ Composite Thin Films on FTO Coated Glass and 3-D Nanospike Structures for Efficient Photoelectrochemical Water Splitting. ACS Applied Materials & Interfaces, 2016, 8, 35315-35322.	8.0	67
193	Co(II) _{1–<i>x</i>} Co(0) _{<i>x×/i>/3</i>} Mn(III) _{2<i>x×/i>/3</i>} S Nanoparticles Supported on B/N-Codoped Mesoporous Nanocarbon as a Bifunctional Electrocatalyst of Oxygen Reduction/Evolution for High-Performance Zinc-Air Batteries. ACS Applied Materials & Amp; Interfaces, 2016. 8, 13348-13359.	8.0	77
194	Nearâ€Infrared Photoresponse of Oneâ€Sided Abrupt MAPbl ₃ /TiO ₂ Heterojunction through a Tunneling Process. Advanced Functional Materials, 2016, 26, 8545-8554.	14.9	23
195	Amorphous Semiconductor Nanowires Created by Site-Specific Heteroatom Substitution with Significantly Enhanced Photoelectrochemical Performance. ACS Nano, 2016, 10, 7882-7891.	14.6	32
196	A PCBM Electron Transport Layer Containing Small Amounts of Dual Polymer Additives that Enables Enhanced Perovskite Solar Cell Performance. Advanced Science, 2016, 3, 1500353.	11.2	67
197	Porous FeNi oxide nanosheets as advanced electrochemical catalysts for sustained water oxidation. Journal of Materials Chemistry A, 2016, 4, 14939-14943.	10.3	63
198	Shining carbon dots: Synthesis and biomedical and optoelectronic applications. Nano Today, 2016, 11, 565-586.	11.9	563

#	Article	IF	CITATIONS
199	An amorphous precursor route to the conformable oriented crystallization of CH ₃ NH ₃ PbBr ₃ in mesoporous scaffolds: toward efficient and thermally stable carbon-based perovskite solar cells. Journal of Materials Chemistry A, 2016, 4, 12897-12912.	10.3	77
200	Hierarchical Dualâ€Scaffolds Enhance Charge Separation and Collection for High Efficiency Semitransparent Perovskite Solar Cells. Advanced Materials Interfaces, 2016, 3, 1600484.	3.7	40
201	Designing new fullerene derivatives as electron transporting materials for efficient perovskite solar cells with improved moisture resistance. Nano Energy, 2016, 30, 341-346.	16.0	72
202	Colloidal Precursor-Induced Growth of Ultra-Even CH3NH3PbI3 for High-Performance Paintable Carbon-Based Perovskite Solar Cells. ACS Applied Materials & Interfaces, 2016, 8, 30184-30192.	8.0	53
203	A General and Mild Approach to Controllable Preparation of Manganeseâ€Based Micro―and Nanostructured Bars for High Performance Lithiumâ€Ion Batteries. Angewandte Chemie - International Edition, 2016, 55, 3667-3671.	13.8	89
204	Dualâ€Ðoped Molybdenum Trioxide Nanowires: A Bifunctional Anode for Fiber‧haped Asymmetric Supercapacitors and Microbial Fuel Cells. Angewandte Chemie - International Edition, 2016, 55, 6762-6766.	13.8	230
205	Understanding the relationship between ion migration and the anomalous hysteresis in high-efficiency perovskite solar cells: A fresh perspective from halide substitution. Nano Energy, 2016, 26, 620-630.	16.0	167
206	High-performance, stable and low-cost mesoscopic perovskite (CH3NH3PbI3) solar cells based on poly(3-hexylthiophene)-modified carbon nanotube cathodes. Frontiers of Optoelectronics, 2016, 9, 71-80.	3.7	42
207	Recent progress in the development of anodes for asymmetric supercapacitors. Journal of Materials Chemistry A, 2016, 4, 4634-4658.	10.3	154
208	Investigating the role of the π-bridge characteristics in donor–π-spacer–acceptor type dyes for solar cell application: a theoretical study. Theoretical Chemistry Accounts, 2016, 135, 1.	1.4	5
209	Designing nanobowl arrays of mesoporous TiO ₂ as an alternative electron transporting layer for carbon cathode-based perovskite solar cells. Nanoscale, 2016, 8, 6393-6402.	5.6	89
210	Transition metal based layered double hydroxides tailored for energy conversion and storage. Materials Today, 2016, 19, 213-226.	14.2	464
211	A computational study on surface-enhanced Raman spectroscopy of para-substituted Benzenethiol derivatives adsorbed on gold nanoclusters. Spectrochimica Acta - Part A: Molecular and Biomolecular Spectroscopy, 2016, 152, 278-287.	3.9	17
212	Interface and Nanostructural Engineering of Low-cost, Efficient and Stable Perovskite Solar Cells. Materials Research Society Symposia Proceedings, 2015, 1771, 171-179.	0.1	1
213	Multicolor fluorescent graphene quantum dots colorimetrically responsive to all-pH and a wide temperature range. Nanoscale, 2015, 7, 11727-11733.	5.6	187
214	Mesoporous SnO ₂ single crystals as an effective electron collector for perovskite solar cells. Physical Chemistry Chemical Physics, 2015, 17, 18265-18268.	2.8	82
215	A sensitive SERS substrate based on Au/TiO2/Au nanosheets. Spectrochimica Acta - Part A: Molecular and Biomolecular Spectroscopy, 2015, 142, 50-54.	3.9	23
216	Self‣ustained Cycle of Hydrolysis and Etching at Solution/Solid Interfaces: A General Strategy To Prepare Metal Oxide Microâ€∤Nanostructured Arrays for Highâ€Performance Electrodes. Angewandte Chemie - International Edition, 2015, 54, 3932-3936.	13.8	34

#	Article	IF	CITATIONS
217	Highâ€Performance Grapheneâ€Based Hole Conductorâ€Free Perovskite Solar Cells: Schottky Junction Enhanced Hole Extraction and Electron Blocking. Small, 2015, 11, 2269-2274.	10.0	233
218	Electrochemical synthesis of small-sized red fluorescent graphene quantum dots as a bioimaging platform. Chemical Communications, 2015, 51, 2544-2546.	4.1	297
219	Strongly coupled metal oxide nanorod arrays with graphene nanoribbons and nanosheets enable novel solid-state hybrid cells. Journal of Power Sources, 2015, 283, 95-103.	7.8	11
220	A multifunctional C + epoxy/Ag-paint cathode enables efficient and stable operation of perovskite solar cells in watery environments. Journal of Materials Chemistry A, 2015, 3, 16430-16434.	10.3	77
221	Single crystalline indene-C ₆₀ bisadduct: isolation and application in polymer solar cells. Journal of Materials Chemistry A, 2015, 3, 14991-14995.	10.3	38
222	A scalable electrodeposition route to the low-cost, versatile and controllable fabrication of perovskite solar cells. Nano Energy, 2015, 15, 216-226.	16.0	207
223	Hybrid Halide Perovskite Solar Cell Precursors: Colloidal Chemistry and Coordination Engineering behind Device Processing for High Efficiency. Journal of the American Chemical Society, 2015, 137, 4460-4468.	13.7	586
224	Preparation and characterization of ZnO tetrapods and octapods. Materials Letters, 2015, 154, 103-106.	2.6	1
225	Hysteresis-free multi-walled carbon nanotube-based perovskite solar cells with a high fill factor. Journal of Materials Chemistry A, 2015, 3, 24226-24231.	10.3	217
226	Origin of the Different Photoelectrochemical Performance of Mesoporous BiVO ₄ Photoanodes between the BiVO ₄ and the FTO Side Illumination. Journal of Physical Chemistry C, 2015, 119, 23350-23357.	3.1	70
227	Metallic Iron–Nickel Sulfide Ultrathin Nanosheets As a Highly Active Electrocatalyst for Hydrogen Evolution Reaction in Acidic Media. Journal of the American Chemical Society, 2015, 137, 11900-11903.	13.7	609
228	High performance inverted structure perovskite solar cells based on a PCBM:polystyrene blend electron transport layer. Journal of Materials Chemistry A, 2015, 3, 9098-9102.	10.3	192
229	Iron-doping-enhanced photoelectrochemical water splitting performance of nanostructured WO ₃ : a combined experimental and theoretical study. Nanoscale, 2015, 7, 2933-2940.	5.6	171
230	Co intake mediated formation of ultrathin nanosheets of transition metal LDH—an advanced electrocatalyst for oxygen evolution reaction. Chemical Communications, 2015, 51, 1120-1123.	4.1	195
231	Magnetic-field-assisted aerosol pyrolysis synthesis of iron pyrite sponge-like nanochain networks as cost-efficient counter electrodes in dye-sensitized solar cells. Journal of Materials Chemistry A, 2014, 2, 5508-5515.	10.3	22
232	Epitaxial Growth of ZnO Nanodisks with Large Exposed Polar Facets on Nanowire Arrays for Promoting Photoelectrochemical Water Splitting. Small, 2014, 10, 4760-4769.	10.0	61
233	Threeâ€Dimensional Graphitized Carbon Nanovesicles for Highâ€Performance Supercapacitors Based on Ionic Liquids. ChemSusChem, 2014, 7, 777-784.	6.8	28
234	Direct observation of <i>p,p</i> ′â€dimercaptoazobenzene produced from <i>p</i> â€aminothiophenol and <i>p</i> â€nitrothiophenol on Cu ₂ 0 nanoparticles by surfaceâ€enhanced Raman spectroscopy. Journal of Raman Spectroscopy, 2014, 45, 7-14.	2.5	24

#	Article	IF	CITATIONS
235	Effects of Fullerene Bisadduct Regioisomers on Photovoltaic Performance. Advanced Functional Materials, 2014, 24, 158-163.	14.9	104
236	Synthesis of ZnO nanorod arrays on Zn substrates by a gas–solution–solid method and their application as an ammonia sensor. Journal of Materials Science, 2014, 49, 347-352.	3.7	9
237	Coupling surface plasmon resonance of gold nanoparticles with slow-photon-effect of TiO2 photonic crystals for synergistically enhanced photoelectrochemical water splitting. Energy and Environmental Science, 2014, 7, 1409.	30.8	288
238	Design Hierarchical Electrodes with Highly Conductive NiCo ₂ S ₄ Nanotube Arrays Grown on Carbon Fiber Paper for High-Performance Pseudocapacitors. Nano Letters, 2014, 14, 831-838.	9.1	1,045
239	Surrounding media sensitive photoluminescence of boron-doped graphene quantum dots for highly fluorescent dyed crystals, chemical sensing and bioimaging. Carbon, 2014, 70, 149-156.	10.3	232
240	MoSe ₂ nanosheets and their graphene hybrids: synthesis, characterization and hydrogen evolution reaction studies. Journal of Materials Chemistry A, 2014, 2, 360-364.	10.3	564
241	Improving the photo current of the [60]PCBM/P3HT photodetector device by using wavelength-matched photonic crystals. Journal of Materials Chemistry C, 2014, 2, 1500.	5.5	19
242	CuO nanostructures: Synthesis, characterization, growth mechanisms, fundamental properties, and applications. Progress in Materials Science, 2014, 60, 208-337.	32.8	1,086
243	Polyfluorene Derivatives are Highâ€Performance Organic Holeâ€Transporting Materials for Inorganicâ"Organic Hybrid Perovskite Solar Cells. Advanced Functional Materials, 2014, 24, 7357-7365.	14.9	172
244	Ag2S nanocaps from AgBr nanoplates: Template symmetry breaking synthesis induced by the polar surfaces. CrystEngComm, 2014, 16, 4940.	2.6	5
245	Cost-efficient clamping solar cells using candle soot for hole extraction from ambipolar perovskites. Energy and Environmental Science, 2014, 7, 3326-3333.	30.8	272
246	Selective laser sintering of TiO ₂ nanoparticle film on plastic conductive substrate for highly efficient flexible dye-sensitized solar cell application. Journal of Materials Chemistry A, 2014, 2, 4566-4573.	10.3	40
247	A three-dimensional hexagonal fluorine-doped tin oxide nanocone array: a superior light harvesting electrode for high performance photoelectrochemical water splitting. Energy and Environmental Science, 2014, 7, 3651-3658.	30.8	103
248	Dithieno[3,2-b:2′,3′-d]pyran-containing organic Dâ€″π–A sensitizers for dye-sensitized solar cells. RSC Advances, 2014, 4, 62472-62475.	3.6	7
249	High-Rate, Ultralong Cycle-Life Lithium/Sulfur Batteries Enabled by Nitrogen-Doped Graphene. Nano Letters, 2014, 14, 4821-4827.	9.1	683
250	Liquid phase deposition of TiO ₂ nanolayer affords CH ₃ NH ₃ PbI ₃ /nanocarbon solar cells with high open-circuit voltage. Faraday Discussions, 2014, 176, 271-286.	3.2	54
251	Unveiling Two Electron-Transport Modes in Oxygen-Deficient TiO ₂ Nanowires and Their Influence on Photoelectrochemical Operation. Journal of Physical Chemistry Letters, 2014, 5, 2890-2896.	4.6	55
252	Highly dispersible and charge-tunable magnetic Fe ₃ O ₄ nanoparticles: facile fabrication and reversible binding to GO for efficient removal of dye pollutants. Journal of Materials Chemistry A, 2014, 2, 15763-15767.	10.3	23

#	Article	IF	CITATIONS
253	Inkjet Printing and Instant Chemical Transformation of a CH ₃ NH ₃ Pbl ₃ /Nanocarbon Electrode and Interface for Planar Perovskite Solar Cells. Angewandte Chemie - International Edition, 2014, 53, 13239-13243.	13.8	370
254	Highâ€Performance Holeâ€Extraction Layer of Sol–Gelâ€Processed NiO Nanocrystals for Inverted Planar Perovskite Solar Cells. Angewandte Chemie - International Edition, 2014, 53, 12571-12575.	13.8	355
255	Space-Confined Growth of MoS ₂ Nanosheets within Graphite: The Layered Hybrid of MoS ₂ and Graphene as an Active Catalyst for Hydrogen Evolution Reaction. Chemistry of Materials, 2014, 26, 2344-2353.	6.7	634
256	A Strongly Coupled Graphene and FeNi Double Hydroxide Hybrid as an Excellent Electrocatalyst for the Oxygen Evolution Reaction. Angewandte Chemie - International Edition, 2014, 53, 7584-7588.	13.8	694
257	Solution-Processed, Barrier-Confined, and 1D Nanostructure Supported Quasi-quantum Well with Large Photoluminescence Enhancement. ACS Nano, 2014, 8, 3771-3780.	14.6	6
258	Efficiency Enhancement of Perovskite Solar Cells through Fast Electron Extraction: The Role of Graphene Quantum Dots. Journal of the American Chemical Society, 2014, 136, 3760-3763.	13.7	688
259	Efficient Photoelectrochemical Water Splitting with Ultrathin films of Hematite on Three-Dimensional Nanophotonic Structures. Nano Letters, 2014, 14, 2123-2129.	9.1	307
260	High performance flexible solid-state asymmetric supercapacitors from MnO ₂ /ZnO core–shell nanorods//specially reduced graphene oxide. Journal of Materials Chemistry C, 2014, 2, 1331-1336.	5.5	266
261	Effect of nitrogen doping on the photo-catalytic properties of nitrogen doped ZnO tetrapods. Materials Letters, 2014, 131, 64-66.	2.6	17
262	Near Field Enhanced Photocurrent Generation in P-type Dye-Sensitized Solar Cells. Scientific Reports, 2014, 4, 3961.	3.3	24
263	MFe ₂ O ₄ and MFe@Oxide Core–Shell Nanoparticles Anchored on Nâ€Doped Graphene Sheets for Synergistically Enhancing Lithium Storage Performance and Electrocatalytic Activity for Oxygen Reduction Reactions. Particle and Particle Systems Characterization, 2013, 30, 893-904.	2.3	25
264	Synthesis of Li-doped Co3O4 truncated octahedra with improved performances in CO oxidation and lithium ion batteries. Science China Technological Sciences, 2013, 56, 8-12.	4.0	6
265	Highly conductive polymer composites from room-temperature ionic liquid cured epoxy resin: effect of interphase layer on percolation conductance. RSC Advances, 2013, 3, 1916-1921.	3.6	23
266	Oneâ€pot Synthesis of Mesoporous TiO ₂ from Selfâ€Assembled Sol Particles and Its Application as Mesoscopic Photoanodes of Dyeâ€Sensitized Solar Cells. ChemPlusChem, 2013, 78, 647-655.	2.8	2
267	All-solid-state hybrid solar cells based on a new organometal halide perovskite sensitizer and one-dimensional TiO2 nanowire arrays. Nanoscale, 2013, 5, 3245.	5.6	401
268	A Quasi-Quantum Well Sensitized Solar Cell with Accelerated Charge Separation and Collection. Journal of the American Chemical Society, 2013, 135, 9531-9539.	13.7	105
269	Highly conductive die attach adhesive from percolation control and its applications in light-emitting device thermal management. Applied Physics Letters, 2013, 102, .	3.3	4
270	Self-assembly of Ni2P nanowires as high-efficiency electrocatalyst for dye-sensitized solar cells. MRS Communications, 2012, 2, 97-99.	1.8	7

#	Article	IF	CITATIONS
271	Effects of Alkoxy Chain Length in Alkoxy-Substituted Dihydronaphthyl-Based [60]Fullerene Bisadduct Acceptors on Their Photovoltaic Properties. ACS Applied Materials & Interfaces, 2012, 4, 5966-5973.	8.0	27
272	Facile synthesis of water-soluble, highly fluorescent graphene quantum dots as a robust biological label for stem cells. Journal of Materials Chemistry, 2012, 22, 7461.	6.7	667
273	Coordination Polyhedra: A Probable Basic Growth Unit in Solution for the Crystal Growth of Inorganic Nonmetallic Nanomaterials?. Crystal Growth and Design, 2012, 12, 2653-2661.	3.0	14
274	Self-Limiting Assembly of Two-Dimensional Domains from Graphene Oxide at the Air/Water Interface. Journal of Physical Chemistry C, 2012, 116, 19018-19024.	3.1	21
275	A composite material of uniformly dispersed sulfur on reduced graphene oxide: Aqueous one-pot synthesis, characterization and excellent performance as the cathode in rechargeable lithium-sulfur batteries. Nano Research, 2012, 5, 726-738.	10.4	116
276	Branched ZnO nanostructures as building blocks of photoelectrodes for efficient solar energy conversion. Physical Chemistry Chemical Physics, 2012, 14, 10872.	2.8	55
277	Facile Ultrasonic Synthesis of CoO Quantum Dot/Graphene Nanosheet Composites with High Lithium Storage Capacity. ACS Nano, 2012, 6, 1074-1081.	14.6	475
278	Bio-inspired synthesis of NaCl-type CoxNi1â^'xO (0 ≤ < 1) nanorods on reduced graphene oxide sheets and screening for asymmetric electrochemical capacitors. Journal of Materials Chemistry, 2012, 22, 12253.	6.7	194
279	Dihydronaphthyl-based [60]fullerene bisadducts for efficient and stable polymer solar cells. Chemical Communications, 2012, 48, 425-427.	4.1	122
280	Highly Efficient and Thermally Stable Polymer Solar Cells with Dihydronaphthylâ€Based [70]Fullerene Bisadduct Derivative as the Acceptor. Advanced Functional Materials, 2012, 22, 2187-2193.	14.9	104
281	Perpendicularly aligned carbon nanotube/olefin composite films for the preparation of graphene nanomaterials. Journal of Materials Chemistry, 2012, 22, 16209.	6.7	4
282	A double layered photoanode made of highly crystalline TiO2 nanooctahedra and agglutinated mesoporous TiO2 microspheres for high efficiency dye sensitized solar cells. Energy and Environmental Science, 2011, 4, 2168.	30.8	146
283	Polymorphic and morphological selection of CaCO3 by magnesium-assisted mineralization in gelatin: magnesium-rich spheres consisting of centrally aligned calcite nanorods and their good mechanical properties. CrystEngComm, 2011, 13, 2472.	2.6	14
284	Unveiling the critical process in which organic molecules control the polymorphism of magnesium-containing calcium carbonate: the early nucleation of amorphous precursors or the subsequent amorphous to crystalline transformations?. CrystEngComm, 2011, 13, 6223.	2.6	7
285	Sequential crystallization of sea urchin-like bimetallic (Ni, Co) carbonate hydroxide and its morphology conserved conversion to porous NiCo2O4 spinel for pseudocapacitors. RSC Advances, 2011, 1, 588.	3.6	289
286	High performance supercapacitors based on highly conductive nitrogen-doped graphene sheets. Physical Chemistry Chemical Physics, 2011, 13, 12554.	2.8	273
287	Electrochemically generated fluorescent fullerene[60] nanoparticles as a new and viable bioimaging platform. Journal of Materials Chemistry, 2011, 21, 819-823.	6.7	41
288	Nanowires of α- and β-Bi ₂ O ₃ : phase-selective synthesis and application in photocatalysis. CrystEngComm, 2011, 13, 1843-1850.	2.6	169

#	Article	IF	CITATIONS
289	Photoluminescence of colloidal CdSe nano-tetrapods and quantum dots in oxygenic and oxygen-free environments. Applied Physics A: Materials Science and Processing, 2011, 103, 279-284.	2.3	6
290	Dye-sensitized solar cells based on ZnO nanotetrapods. Frontiers of Optoelectronics in China, 2011, 4, 24-44.	0.2	10
291	Biomimetic Synthesis, Hierarchical Assembly and Mechanical Properties of Calcite/Chitosan Composites in a Three-Dimensional Chitosan Scaffold. Advanced Engineering Materials, 2011, 13, B32-B40.	3.5	10
292	Electrorheological characterization of ultrathin titanium dioxide nanorods solutions using microfluidics. , 2010, , .		0
293	Synthesis and high lithium electroactivity of rutile TiO <inf>2</inf> @C nanorods. , 2010, , .		1
294	Template-free solution growth of highly regular, crystal orientation-ordered C ₆₀ nanorod bundles. Journal of Materials Chemistry, 2010, 20, 953-956.	6.7	21
295	Synthesis of Size-Tunable Anatase TiO ₂ Nanospindles and Their Assembly into Anatase@Titanium Oxynitride/Titanium Nitrideâ^'Graphene Nanocomposites for Rechargeable Lithium Ion Batteries with High Cycling Performance. ACS Nano, 2010, 4, 6515-6526.	14.6	262
296	Facile hydrothermal preparation of hierarchically assembled, porous single-crystalline ZnO nanoplates and their application in dye-sensitized solar cells. Journal of Materials Chemistry, 2010, 20, 1001-1006.	6.7	137
297	Synthesis and characterization of angstrom-scale anatase titania atomic wires. , 2010, , .		0
298	A novel nanostructured spinel ZnCo2O4 electrode material: morphology conserved transformation from a hexagonal shaped nanodisk precursor and application in lithium ion batteries. Journal of Materials Chemistry, 2010, 20, 4439.	6.7	185
299	Hollow calcite crystals with complex morphologies formed from amorphous precursors and regulated by surfactant micellar structures. CrystEngComm, 2010, 12, 3296.	2.6	13
300	Highly Selective and Sensitive Detection of Dopamine in the Presence of Excessive Ascorbic Acid Using Electrodes Modified with C ₆₀ â€Functionalized Multiwalled Carbon Nanotube Films. Electroanalysis, 2009, 21, 2660-2666.	2.9	31
301	Electrochemistry of Sc3N@C78 embedded in didodecyldimethylammonium bromide films in aqueous solution. Mikrochimica Acta, 2009, 165, 45-52.	5.0	0
302	In Situ Fabrication of Inorganic Nanowire Arrays Grown from and Aligned on Metal Substrates. Accounts of Chemical Research, 2009, 42, 1617-1627.	15.6	95
303	Synthesis of Angstrom-Scale Anatase Titania Atomic Wires. ACS Nano, 2009, 3, 1025-1031.	14.6	78
304	General surfactant-free synthesis of MTiO3 (M = Ba, Sr, Pb) perovskite nanostrips. Journal of Materials Chemistry, 2009, 19, 976.	6.7	61
305	CdS-Ag nanocomposite arrays: enhanced electro-chemiluminescence but quenched photoluminescence. Journal of Materials Chemistry, 2009, 19, 3841.	6.7	56
306	Electrochemical route to the preparation of highly dispersed composites of ZnO/carbon nanotubes with significantly enhanced electrochemiluminescence from ZnO. Journal of Materials Chemistry, 2008, 18, 4964.	6.7	90

#	Article	IF	CITATIONS
307	Additive-Mediated Splitting of Lanthanide Orthovanadate Nanocrystals in Water: Morphological Evolution from Rods to Sheaves and to Spherulites. Crystal Growth and Design, 2008, 8, 4432-4439.	3.0	84
308	Preparation of Novel Cuprous Oxideâ^'Fullerene[60] Coreâ^'Shell Nanowires and Nanoparticles via a Copper(I)-Assisted Fullerene-Polymerization Reaction. Journal of Physical Chemistry C, 2008, 112, 7110-7118.	3.1	20
309	Monodisperse nanocrystals of LnV0 <inf>4</inf> (Ln = Ce, Nd): Controlled synthesis and upconverted avalanche luminescence. , 2008, , .		0
310	FORMATION OF POLARIZED CONTACT LAYERS AND THE GIANT ELECTRORHEOLOGICAL EFFECT. International Journal of Modern Physics B, 2007, 21, 4907-4913.	2.0	5
311	Vertically aligned zinc selenide nanoribbon arrays: microstructure and field emission. Journal Physics D: Applied Physics, 2007, 40, 3587-3591.	2.8	25
312	From cylindrical-channel mesoporous silica to vesicle-like silica with well-defined multilamella shells and large inter-shell mesopores. Journal of Materials Chemistry, 2007, 17, 2839.	6.7	71
313	Emergent methods to synthesize and characterize semiconductor CuO nanoparticles with various morphologies – an overview. Journal of Experimental Nanoscience, 2007, 2, 23-56.	2.4	52
314	FORMATION OF POLARIZED CONTACT LAYERS AND THE GIANT ELECTRORHELOGICAL EFFECT. , 2007, , .		0
315	Growth of novel nanostructured copper oxide (CuO) films on copper foil. Journal of Crystal Growth, 2006, 291, 479-484.	1.5	79
316	Mechanisms of the giant electrorheological effect. Solid State Communications, 2006, 139, 581-588.	1.9	68
317	Wetting-induced electrorheological effect. Journal of Applied Physics, 2006, 99, 106104.	2.5	36
318	Quantitative Non-Covalent Functionalization of Carbon Nanotubes. Journal of Cluster Science, 2006, 17, 599-608.	3.3	21
319	Hydrothermal Synthesis and Optical Properties of ZnO Nanostructured Films Directly Grown from/on Zinc Substrates. Journal of Sol-Gel Science and Technology, 2006, 39, 73-73.	2.4	4
320	Chemical synthesis and magnetic properties of dilute magnetic ZnTe:Cr crystals. Applied Physics Letters, 2006, 89, 092111.	3.3	20
321	CdSe Nano-tetrapods:  Controllable Synthesis, Structure Analysis, and Electronic and Optical Properties. Chemistry of Materials, 2005, 17, 5263-5267.	6.7	114
322	Room temperature growth of CuO nanorod arrays on copper and their application as a cathode in dye-sensitized solar cells. Materials Chemistry and Physics, 2005, 93, 35-40.	4.0	288
323	Hydrothermal Synthesis and Optical Properties of ZnO Nanostructured Films Directly Grown from/on Zinc Substrates. Journal of Sol-Gel Science and Technology, 2005, 36, 227-234.	2.4	22
324	Transport and TEM on the same individual carbon nanotubes and peapods. AIP Conference Proceedings, 2005, , .	0.4	0

#	Article	IF	CITATIONS
325	Controlled p- and n-type doping of Fe2O3 nanobelt field effect transistors. Applied Physics Letters, 2005, 87, 013113.	3.3	114
326	Effects of light illumination on field emission from CuO nanobelt arrays. Applied Physics Letters, 2005, 86, 151107.	3.3	44
327	Nanostructured stars of ZnO microcrystals with intense stimulated emission. Applied Physics Letters, 2005, 87, 163103.	3.3	20
328	The Development of Functional Endohedral Metallofullerene Materials. Fullerenes Nanotubes and Carbon Nanostructures, 2005, 13, 155-158.	2.1	2
329	ZnO Nanobelt Arrays Grown Directly from and on Zinc Substrates:Â Synthesis, Characterization, and Applications. Journal of Physical Chemistry B, 2005, 109, 15303-15308.	2.6	117
330	Controlled Growth of Large-Area, Uniform, Vertically Aligned Arrays of α-Fe2O3Nanobelts and Nanowires. Journal of Physical Chemistry B, 2005, 109, 215-220.	2.6	506
331	Electrical Transport in Dy Metallofullerene Peapods. AIP Conference Proceedings, 2004, , .	0.4	0
332	Transmission electron microscopy and transistor characteristics of the same carbon nanotube. Applied Physics Letters, 2004, 85, 2911-2913.	3.3	27
333	Effects of Aromatic Substitutions on the Photoreactions in Mg•+(C6HnF2X4-n) (X = F, CH3) Complexes:Â Formation and Decomposition of Benzyne Radical Cations. Journal of Physical Chemistry A, 2004, 108, 3356-3366.	2.5	8
334	The giant electrorheological effect in suspensions of nanoparticles. Nature Materials, 2003, 2, 727-730.	27.5	530
335	Synthesis and Characterization of Uniform Arrays of Copper Sulfide Nanorods Coated with Nanolayers of Polypyrrole. Langmuir, 2003, 19, 4420-4426.	3.5	110
336	Controlled Reactions on a Copper Surface:  Synthesis and Characterization of Nanostructured Copper Compound Films. Inorganic Chemistry, 2003, 42, 5005-5014.	4.0	202
337	Synthesis of Cu(OH)2and CuO Nanoribbon Arrays on a Copper Surface. Langmuir, 2003, 19, 5898-5903.	3.5	233
338	Effect of structural parameter on field emission properties of semiconducting copper sulphide nanowire films. Journal of Applied Physics, 2003, 93, 1774-1777.	2.5	39
339	Resonant two-photon ionization spectroscopy of the van der Waals complex C6H5CH3â< N2: Structure, binding energy, intermolecular vibrations, and internal rotation. Journal of Chemical Physics, 2003, 119, 8321-8326.	3.0	3
340	Photo-induced reactions in the ion–molecule complex Mg+–OCNC2H5. Journal of Chemical Physics, 2003, 118, 10455-10460.	3.0	13
341	Temperature dependence of field emission from cupric oxide nanobelt films. Applied Physics Letters, 2003, 83, 746-748.	3.3	165
342	Electrochemical Response of Metallofullerene Films Casted on Electrodes. AIP Conference Proceedings, 2003, , .	0.4	0

#	Article	IF	CITATIONS
343	Photodissociation spectroscopy of the complexes of Mg+ with di- and tri-ethylamine. Journal of Chemical Physics, 2002, 116, 2896-2906.	3.0	20
344	Photo-induced intra-complex reactions in Mg+-2,2,2-trifluoroethanol. Journal of Chemical Physics, 2002, 116, 9690-9696.	3.0	16
345	Field emission from crystalline copper sulphide nanowire arrays. Applied Physics Letters, 2002, 80, 3620-3622.	3.3	191
346	Cu2S/Au Core/Sheath Nanowires Prepared by a Simple Redox Deposition Method. Nano Letters, 2002, 2, 451-454.	9.1	56
347	Thermal oxidation of Cu2S nanowires: A template method for the fabrication of mesoscopic CuxO (x = 1,2) wires. Physical Chemistry Chemical Physics, 2002, 4, 3425-3429.	2.8	84
348	Solution Phase Synthesis of Cu(OH)2Nanoribbons by Coordination Self-Assembly Using Cu2S Nanowires as Precursors. Nano Letters, 2002, 2, 1397-1401.	9.1	192
349	Photoinduced reactions in the Mg+–NHn(CH3)3â^'n complex ions: Effect of the methyl substitution. Journal of Chemical Physics, 2002, 117, 6061-6070.	3.0	14
350	Photoconductivity of poly(N-vinylcarbazole) (PVK) doped with the metallofullerene Dy@C82and the fullerenes C84and C60. Israel Journal of Chemistry, 2001, 41, 45-50.	2.3	2
351	Photodissociation studies of microsolvated metal cation complexes Mg+(NCCH3)n (n=1–4). Journal of Chemical Physics, 2001, 115, 4612-4619.	3.0	20
352	Growth behaviour of straight crystalline copper sulphide nanowires. Advanced Materials for Optics and Electronics, 2000, 10, 39-45.	0.4	28
353	Synthesis and Characterization of Poly(vinylpyrrolidone)-Modified Zinc Oxide Nanoparticles. Chemistry of Materials, 2000, 12, 2268-2274.	6.7	262
354	One-dimensional growth of rock-salt PbS nanocrystals mediated by surfactant/polymer templates. Pure and Applied Chemistry, 2000, 72, 119-126.	1.9	21
355	Photodissociation spectroscopy of Mg+–C6H5X (X=H, F, Cl, Br). Journal of Chemical Physics, 2000, 112, 10236-10246.	3.0	23
356	Photo-induced reactions in mass-selected complexes Mg+(FCH3)n, n=1–4. Journal of Chemical Physics, 2000, 113, 3111-3120.	3.0	20
357	Highly monodisperse polymer-capped ZnO nanoparticles: Preparation and optical properties. Applied Physics Letters, 2000, 76, 2901-2903.	3.3	455
358	Poly(N-vinylcarbazole) (PVK) Photoconductivity Enhancement Induced by Doping with CdS Nanocrystals through Chemical Hybridization. Journal of Physical Chemistry B, 2000, 104, 11853-11858.	2.6	123
359	Magnetic Properties of Heavy Rare-Earth Metallofullerenes M@C82 (M = Gd, Tb, Dy, Ho, and Er). Journal of Physical Chemistry B, 2000, 104, 1473-1482.	2.6	68
360	Photofragmentation studies of small selenium cluster cations Sen+ (n=3–8). Journal of Chemical Physics, 1999, 111, 7837-7843.	3.0	17

#	Article	IF	CITATIONS
361	Resonant two-photon ionization spectra of van der Waals complexes p, m, o-C6H4F2â<⁻NH3(ND3). Journal of Chemical Physics, 1999, 111, 134-139.	3.0	8
362	Synthesis and Characterization of PbS Nanocrystallites in Random Copolymer Ionomers. Chemistry of Materials, 1999, 11, 3365-3369.	6.7	66
363	Film Formation Behavior of the Endohedral Metallofullerene DY@C82. Materials Research Society Symposia Proceedings, 1999, 593, 63.	0.1	0
364	Resonant two-photon ionization and fluorescence excitation studies of o, m-difluorobenzene⋯Ar. Spectral shifts and intermolecular vibrations. Journal of Chemical Physics, 1998, 108, 12-19.	3.0	12
365	Reactions of Lanthanide Cations with Methanol Clusters. Journal of Physical Chemistry A, 1998, 102, 1954-1962.	2.5	17
366	Reactions of Alkaline Earth Metal Ions with Methanol Clusters. Journal of Physical Chemistry A, 1998, 102, 825-840.	2.5	87
367	Scanning Tunneling Microscopy of Ring-Shape Endohedral Metallofullerene (Nd@C82)6,12Clusters. Journal of Physical Chemistry A, 1998, 102, 4411-4413.	2.5	15
368	Dehydrogenation and physisorption of saturated hydrocarbons (n-butane and isobutane) on Nbx+. Journal of Chemical Physics, 1998, 109, 8935-8939.	3.0	6
369	C60 induced photoluminescence of a silica molecular sieve. Applied Physics Letters, 1997, 70, 2619-2621.	3.3	28
370	Twoâ€photon ionization studies of binary aromatic van der Waals clusters: Benzenechlorobenzene and (chlorobenzene)2. Journal of Chemical Physics, 1996, 104, 8843-8851.	3.0	15
371	Resonant twoâ€photon ionization spectra of the van der Waals complexes: C6H5Xâ‹â‹â‹N2 (X=F, Cl, Br). Journal of Chemical Physics, 1996, 105, 5305-5312.	3.0	27
372	Generation of fullerenes and metal–carbon clusters in a pulsed arc cluster ion source (PACIS). Journal of Chemical Physics, 1996, 104, 6577-6581.	3.0	17
373	SYNTHESIS OF La@C2n BY DIRECT La-FULLERENE REACTIONS IN THE LASER-ABLATION PLASMA OF A La2O3/FULLERENE MIXTURE. Surface Review and Letters, 1996, 03, 803-805.	1.1	4
374	Studies of C60â€metal reactions in the laserâ€ablation plasma of C60/M2O3 (M=La, Y, Eu, Gd). Journal of Chemical Physics, 1995, 102, 189-192.	3.0	16
375	Photoionization studies of transition metal clusters: Ionization potentials of ScnO (n=5?36). Zeitschrift Für Physik D-Atoms Molecules and Clusters, 1994, 31, 199-203.	1.0	19
376	Field electron emission from cupric oxide-nanobelt films. , 0, , .		0
377	Transport and TEM on individual nanotubes and nanotube peapods. , 0, , .		0
378	Field emission properties of CuO nanobelts film under light illumination. , 0, , .		0

#	Article	IF	CITATIONS
379	Uniform field emission from CuO nanowires prepared by thermal oxidation method. , 0, , .		0